Published in final edited form as:
J Theor Biol. 2012 July 21; 305C: 45–53. doi:10.1016/j.jtbi.2012.04.009.

Modelling the effects of calcium waves and oscillations on saliva secretion

Laurence Palk[a,*], **James Sneyd**[a], **Kate Patterson**[a], **Trevor J. Shuttleworth**[b], **David I. Yule**[b], **Oliver Maclaren**[c], and **Edmund J. Crampin**[c]

[a]Department of Mathematics, The University of Auckland, Private Bag 92019, Auckland 1142, New Zealand [b]Department of Pharmacology and Physiology and the Centre for Oral Biology, University of Rochester Medical Center, Rochester, NY 14642, USA [c]Auckland Bioengineering Institute and Department of Engineering Science, The University of Auckland, Private Bag 92019, Auckland, New Zealand

Abstract

An understanding of Ca^{2+} signalling in saliva-secreting acinar cells is important, as Ca^{2+} is the second messenger linking stimulation of cells to production of saliva. Ca^{2+} signals effect secretion via the ion channels located both apically and basolaterally in the cell. By approximating Ca^{2+} waves with periodic functions on the apical and basolateral membranes, we isolate individual wave properties and investigate them for their effect on fluid secretion in a mathematical model of the acinar cell. Mean Ca^{2+} concentration is found to be the most significant property in signalling secretion. Wave speed was found to encode a range of secretion rates. Ca^{2+} oscillation frequency and amplitude had little effect on fluid secretion.

Keywords

mathematical model; parotid acinar cell; oscillation frequency; Ca2+ wave speed; calcium signalling

1. Introduction

A problem commonly encountered in quantitative analysis of physiological processes is to determine which experimentally observed behaviours are important to the system and which can be approximated to produce a simple model capable of making predictions and increasing understanding. The salivation process is initiated with an electrical signal from the brain which releases an agonist, ACh, around the acinar cells. This agonist causes production of IP_3 which releases Ca^{2+} from internal stores in the endoplasmic reticulum (ER). Ca^{2+} feedback on IP_3 dynamics can cause periodic oscillations of Ca^{2+} throughout the cytoplasm at a raised baseline. The raised Ca^{2+} concentration opens K^+ and Cl^- channels, causing a change in intracellular and lumenal concentrations of Cl^-, Na^+ and K^+. This concentration change creates an osmotic gradient which leads to increasing fluid secretion

*Corresponding author, Tel: +6499232448, l.palk@math.auckland.ac.nz (Laurence Palk).

from the acinar cells. This process is completed in a great many acinar cells simultaneously and is accompanied by a shrinking of cell volume. Once the fluid is secreted from the acinar cells into the lumen as primary saliva it travels down the parotid ducts where duct cells modify the ionic content before finally being secreted in the mouth.

One mechanism that is particularly well studied is that of the Ca^{2+} dynamics. Ca^{2+} is well known to have an important role as a second messenger in a vast array of cell types. Current models of saliva secretion in the parotid acinar cells by Palk et al. (2010) and Gin et al. (2007) use compartmental models of Ca^{2+} to reproduce experimental results and incorporate into models for saliva secretion. These models assume homogeneous oscillations in Ca^{2+} throughout the cytosol and hence can be modelled using ordinary differential equations. Experimentally, however, Ca^{2+} is not only observed to oscillate but to travel in waves from one membrane to the other. These Ca^{2+} waves have been seen in many cells types including cardiac myocytes, airway smooth muscle, pancreatic acinar cells, neurons (Jaffe (1991)) and parotid acinar cells (Won et al. (2007)). Ca^{2+} waves and oscillations are thought to be able to encode a larger amount of signalling information than a constant Ca^{2+} concentration. Experimental and theoretical evidence suggests that frequency and amplitude are used to encode information in certain cell types (De Koninck and Schulman (1998), Tang and Othmer (1995) and Berridge (1997)). It is not our focus here to investigate the genesis of Ca^{2+} waves, for that see Sneyd et al. (2003). In this paper we seek to investigate how important the properties of Ca^{2+} waves are for controlling the secretion of primary saliva.

Consideration of Ca^{2+} waves, as opposed to homogeneous oscillations, requires consideration of amplitude, mean concentration, frequency and also the wave speed as mechanisms for signalling. Using a detailed spatial model of the Ca^{2+} waves makes it difficult to change one property, say the wave speed, without affecting the others. A spatial modelling approach involves numerically solving partial differential equations throughout the cytosol. Yet as regards saliva secretion, Ca^{2+} acts on ion channels which are located in the apical and basal membranes only. Hence using a spatial model generates far more information than is required and is not the approach taken here. Rather, we approximate Ca^{2+} waves by using periodic functions for Ca^{2+} at the basal and apical membrane. Using this approximation of Ca^{2+} waves we are able to isolate Ca^{2+} wave properties such as frequency, amplitude, wave speed and mean concentration to individually investigate their effect on saliva secretion.

2. Modelling agonist-induced saliva secretion

We use the mathematical model of the parotid acinar cell from Palk et al. (2010). Here saliva secretion is initiated by a raised Ca^{2+} concentration which open K^+ and Cl^- channels. This enables an ionic gradient to be maintained which allows water to flow by osmosis both transcellularly and paracellularly into the lumen. A schematic of the fluid secretion model can be seen in Figure 1.

Being un-buffered we assume that K^+, Cl^- and Na^+ diffuse very quickly and therefore these ionic concentrations are homogeneous throughout the three sub-domains, the interstitium, the cytosol and the lumen.

Transmembrane ion fluxes are driven by Ca^{2+} with the Ca^{2+} concentration at the apical membrane affecting the open probability of the ion channels that reside in the apical membrane and similarly the Ca^{2+} concentration at the basal membrane affecting the ion channels there.

Differential equations are written for the change in Cl^-, K^+, Na^+, cell volume and the apical and basal membrane potentials. These are numerically solved using the *Matlab* routine

ode15s. Foskett (1990) show that volume changes are tightly correlated with changes in cytosolic Cl^-. Our model assumes fluid flow to change instantaneously with ionic changes, and cell volume to follow directly. Details of the model equations are given in Appendix A.

3. Simplified model of Ca^{2+} waves

We consider a periodic Ca^{2+} wave from the apical to basal membrane with a constant period such as seen experimentally by Zimmermann and Walz (1999). At any point throughout the cytosol the concentration of Ca^{2+} will be a periodic function with the same period and a possibly distinct mean and amplitude. We simulate a Ca^{2+} wave with the concentration being a periodic function at both the apical and basal membranes. We can formally write this as follows,

$$C_a = f(t)$$
$$C_b = g(t+\delta)$$

where C_a is the Ca^{2+} concentration at the apical membrane and with C_b the basal Ca^{2+} concentration. Both $f(t)$ and $g(t)$ are assumed to be periodic with the same period T and both attain their minimum values at $t = 0$. The parameter δ is a measure of synchronicity, when $\delta = 0$ Ca^{2+} oscillations are synchronous at the two membranes. When parameter δ is non-zero there is a delay between Ca^{2+} peaking at the apical and basal membrane. This phase-shift can be used to simulate a Ca^{2+} wave with a given speed. Using this model we are free to change individual wave properties, for example the wave amplitude, without affecting the other wave properties.

In Figure 2 we simulate an apical to basal Ca^{2+} wave, periodic with a period of 7 s, where the mean Ca^{2+} concentration and amplitude is the same at both membranes. Here a sine function was used to give the Ca^{2+} profile at both membranes. However, any periodic function with a similar profile to experimentally observed Ca^{2+} oscillations could have been used. For the remainder of the results presented a sine function is used to approximate the oscillations of Ca^{2+} at the apical and basal membranes. The Ca^{2+} concentration C is given by,

$$C = C_{\text{norm}} + C_{\text{amp}} \sin\left(\frac{2\pi(t-\delta)}{\lambda}\right)$$

where C_{norm} is the mean Ca^{2+} concentration, C_{amp} is the amplitude of the Ca^{2+} oscillations, δ allows for the inclusion of a time delay and λ is the period of oscillations.

4. Analysis of the effect of Ca^{2+} wave speed on fluid flow

Previous work has investigated how the frequency of Ca^{2+} oscillations may encode signalling information in the phosphorylation of a cellular substrate by protein kinase, Goldbeter et al. (1990), and in hepatocytes, Larsen et al. (2004). We investigate the effect of wave speed on saliva secretion by varying the time difference between the peak in Ca^{2+} at the apical and basal membranes. Experimentally, Won et al. (2007) report a wave-speed of 27.81 μm/s with Ca^{2+} peaking at the apical membrane approximately 1 second before the basal membrane. These measurements suggest the distance between the two membranes is 27.81 μm: for simplification this work uses a distance of 25 μm between membranes.

In Figure 2 we numerically simulate an apical to basal Ca^{2+} wave having a 1 second time difference between the apical and basal Ca^{2+} peaks. With our assumed cell size of 25 μm from the apical to basal membrane this is equivalent to a wave speed of 25 μm/s. If instead we ran a simulation with a 2 second time between the apical and basal membrane peak in Ca^{2+} this would approximate a wave speed of 12.5 μm/s, assuming the same cell size. Using this idea of changing the time between apical and basal Ca^{2+} peaks we can simulate a range of wave speeds and observe the effect on secretion.

In Figure 3 the effect of the time between apical and basal Ca^{2+} peak can be seen on the average fluid flow rate. It is shown that maximum secretion occurs when the time difference is zero, implying synchronous Ca^{2+} oscillations at the two-membranes, or equivalently a homogeneous rise and fall of Ca^{2+} throughout the cytosol. A minimum secretion rate occurs at a time difference of 3.5 seconds. This is a time difference of exactly half the oscillation period and oscillations at the two membranes are out of phase.

For this result, and the remainder of the analysis, a sinusoidal function was used to approximate the Ca^{2+} oscillations at each membrane. However the same result can be reproduced for several different periodic functions at both membranes. A mathematical argument that a local maximum occurs when oscillations are synchronous for any periodic function is given in Appendix B.

The result that synchronous oscillations are most efficient appears to suggest that the experimentally observed Ca^{2+} waves seen by Won et al. (2007), with a 1 second time difference between apical and basal Ca^{2+} peak, are less than efficient at signalling saliva secretion. There are, however, some assumptions made in the analysis above that we now explore. In particular the model currently has all ion channels operating at steady state. However, experimentally the ion channels have a time dependence. We will address this model shortfall in the following section.

5. Time-dependent Cl^- channel gating

In Arreola et al. (1996) the Cl^- channels are found to react very quickly to changes in Ca^{2+} at physiologically realistic membrane potentials and Ca^{2+} concentrations. This quick opening and closing led us to initially use a steady-state model for the Cl^- channel. We investigate whether adding the time dependence of the Cl^- channel to the model affects the results relating to fluid secretion.

In Arreola et al. (1996) a four-state model is given for the Cl^- channel with three closed and one open state as seen below,

$$C_1 \underset{\beta_1}{\overset{\alpha_1 Ca}{\rightleftharpoons}} C_2 \underset{\beta_1}{\overset{\alpha_1 Ca}{\rightleftharpoons}} C3 \underset{\beta_2}{\overset{\alpha_2}{\rightleftharpoons}} O.$$

Rates α_1 and β_1 are faster than α_2 and β_2 and their dependence on Ca^{2+} is not given explicitly in Arreola et al. (1996). Hence we simplify this model to a 2-state model using a rapid equilibrium approximation to group the three closed states, C_1, C_2 and C_3 into one new closed state C.

$$C \underset{\beta_2}{\overset{\alpha}{\rightleftharpoons}} O$$

This two-state model simplification approximates the experimental data well (result not shown). Applying the two-state reduction we get a differential equation for the fraction of open Cl^- channels,

$$\frac{dO}{dt}=\alpha C-\beta_2 O$$

Here β_2 is the same reverse rate as seen in Arreola et al. (1996). The forward reaction rate, a, given in terms of the original rates K_1, K_2 and a_2 in Arreola et al. (1996), is shown below.

$$\alpha=\alpha_2/\left(1+\frac{K_1}{C_a}+\frac{K_1^2}{C_a^2}\right)$$

Here,

$$K_1=214\exp\left(\frac{-0.13FV_a}{RT}\right)nM,$$

$$K_2=0.58\exp\left(\frac{-0.24FV_a}{RT}\right),$$

$\beta_2 = K_2 a_2\ s^{-1}$, $a_2 = 4.5\ s^{-1}$ and C_a is the Ca^{2+} concentration at the apical membrane. V_a is the membrane potential of the apical membrane. The total current through the Cl^- channels is then given by

$$I_{Cl}=g_{cl}O(V_a-V_{Cl}),$$

where g_{Cl} = 31.4 nS is the maximum whole cell conductance found by Arreola et al. (1996). V_{Cl} is the Nernst potential given by

$$V_{Cl}=\frac{RT}{z_{Cl}F}\log\left(\frac{[Cl]_l}{[Cl]_i}\right),$$

where $[Cl]_l$ and $[Cl]_i$ are the Cl^- concentrations in the lumen and cytosol respectively and $z_{Cl} = -1$ is the valence of Cl^-, $R = 8.315$ J mol^{-1} K^{-1}, $T = 310$ K and $F = 96490$ C mol^{-1}.

5.1. The effect of wave speed on fluid secretion rate in a model with time-dependent Cl^- channels

The effect of wave speed on fluid flow is investigated using the same method of varying the time difference between the apical and basal Ca^{2+} peaks described in Section 4. When time dependence of the Cl^- channel is added to the model we find that a maximum secretion rate

occurs with a small positive time difference between the Ca^{2+} peaking at the apical and basal membranes (see Figure 4). Ca^{2+} waves are simulated with a sinusoidal function with mean 150 nM, amplitude 100 nM and a period of 7 seconds.

In Figure 4 it can be seen that maximum secretion occurs when the Ca^{2+} wave peaks at the apical membrane 0.2 s before the basal membrane. This roughly equates to an apical to basal wave with a speed of 125 μm/s, assuming a cell size of 25 μm from apical to basal membrane. This is much faster than the observed wave speed of 27.81 μm/s seen by Won et al. (2007).

5.2. The effect of wave period on fluid secretion rate in a model with time-dependent Cl^- channels

In Figure 5 a sinusoidal function is used to simulate Ca^{2+} at the two membranes with a mean of 100 nM and an amplitude of 50 nM.

Figure 5 shows that as the period of the Ca^{2+} waves is increased the average saliva secretion rate increases. If Ca^{2+} oscillates quickly the time-dependent Cl^- channel will lag behind the current Ca^{2+} concentration. This results in less than maximum fluid flow. As the Ca^{2+} oscillation period is increased we find that fluid flow reaches a maximum. It should be noted that the rate of secretion changes very little despite large changes in oscillation period with the least efficient rate being only 96% of the most efficient period.

5.3. The effect of mean Ca^{2+} on fluid secretion rate in a model with time-dependent Cl^- channels

The effect of mean Ca^{2+} on fluid flow is seen in Figure 6. As the mean Ca^{2+} concentration increases the amount of secretion increases. The profile of fluid flow as Ca^{2+} increases takes a sigmoidal shape, initially increasing rapidly at low Ca^{2+} concentrations and levelling off as the ion channel open probability approaches 1. A very large difference is observed in secretion rates with a high Ca^{2+} concentration secreting almost 10 times the volume of low concentrations.

5.4. The effect of oscillation amplitude on fluid secretion rate in a model with time-dependent Cl^- channels

The effect of oscillation amplitude on fluid flow is investigated. With a mean Ca^{2+} concentration of 100 nM, increasing the amplitude of oscillations increases the rate of secretion. This can be seen in Figure 7a. If instead the mean Ca^{2+} is increased to 300 nM the opposite is true, Figure 7b, with increasing oscillation amplitude reducing secretion. This result can be explained by the profile of fluid flow with mean Ca^{2+} seen in Figure 6. At low Ca^{2+} concentrations the function is convex. Jensen's inequality states

$$E[f(x)] \geq f(E[x])$$

where E is the expectation and f is a convex function. If we consider an oscillating function of Ca^{2+}, this inequality says that the average secretion rate for some oscillating function of Ca^{2+} is greater than the rate of secretion at the mean Ca^{2+} concentration. Or equivalently, we expect a larger amplitude to give us greater secretion than a constant Ca^{2+} concentration.

With a larger mean Ca^{2+} concentration the profile of secretion with Ca^{2+} becomes concave and the converse is true with larger amplitude causing a reduction in secretion. At a mean

Ca^{2+} concentration of around 120 nM the secretion rate as a function of Ca^{2+} is neither convex or concave. Here amplitude has no significant effect on secretion (result not shown).

6. Discussion

Ca^{2+} signals involving oscillations are commonly found in biological systems, and are thought to enable a larger bandwidth of signalling. We have found that each of the investigated properties of Ca^{2+} waves are capable of altering the rate of saliva secretion to differing degrees.

We find Ca^{2+} oscillation frequency to be inefficient at regulating secretion rate, with only a 4% change in secretion over a large range of frequencies. Any difference in secretion is due to the time-dependence of the Cl^- channel as no change is observed when this is absent from the model. Gray (1988) find that given a large range of applied agonist concentrations the parotid acinar cells oscillated with a reasonably constant frequency, potentially supporting the idea that frequency encoding is unimportant in the parotid acinar cell. It is worth noting the shape of Figure 5. As the period is increased a plateau is reached. Bruce et al. (2002) report 7–11 Ca^{2+} oscillations per minute in parotid acinar cells giving a period of 5.5–8.5 seconds. This physiologically realistic range for oscillations lies just at the start of the plateau maximising efficiency of secretion.

As the Ca^{2+} wave speed is changed a noticeable change in secretion rate occurs with the least efficient wave speed secreting 83% of the maximum secretion rate that is obtained with the most efficient wave speed. Our model with time-dependent Cl^- channels predicts apical to basal Ca^{2+} waves to be the most efficient, however the most efficient secretion is predicted for a wave speed much faster than observed experimentally by Won et al. (2007). The model used for this analysis has Cl^- channels in the apical membrane and K^+ in the basal membrane. There is evidence, both experimental and theoretical (Almassy et al. (2012) and Palk et al. (2010)) that apical K^+ channels are found in parotid acinar cells. These K^+ channels are thought to be of the maxi-K type. It is possible that the addition of these K^+ channels to the model with their time dependence could make slower wave speeds more efficient to parotid acinar cell function. Future work would require a detailed study of the activation of maxi-K channels by Ca^{2+} in order for this to be properly resolved.

The experimentally observed wave speed of 27.81 μm/s seen by Won et al. (2007) is found to remain roughly constant in parotid acinar cells for varying amounts of stimulation, and therefore it seems unlikely that wave speed is used as a signalling mechanism. This wave speed is very similar to Ca^{2+} waves observed in other mammalian cell types by Jaffe (1991), with only cardiac myocytes displaying much greater wave speeds. It seems possible that a similar wave generation mechanism in different cell types might limit wave speeds to this narrow range. One might conjecture that Ca^{2+} waves travel at a speed which maximises fluid secretion or, alternatively, that the ion channels responsible for fluid regulation have adapted to maximise secretion for this constrained wave speed.

The effect of Ca^{2+} oscillation amplitude on secretion is dependent on the mean Ca^{2+} concentration, with increasing amplitude increasing secretion at low Ca^{2+} concentrations and decreasing secretion as the mean Ca^{2+} increases. Gray (1988) reports a large range of oscillation amplitudes seen experimentally and thus it is unclear what role amplitude might have in signalling.

By far the most significant mechanism for signalling is the mean Ca^{2+} concentration. Here the flow rate for low Ca^{2+} concentration is less than 10% what is seen for the highest concentration. Foskett and Melvin (1989) find a resting level of Ca^{2+} as 59 nM, increasing to 474 nM when stimulated with carbachol. According to our model this would result in a

10-fold increase in secretion. Experimentally an increase of between 6 and 13 fold is seen between resting and stimulated salivary glands, Ben-Aryeh et al. (1986) and Heft and Baum (1984).

By avoiding a detailed spatial model, wave properties are easily isolated and investigated for their effect on secretion. Several assumptions are made in using this simplified approach. Changing a global variable, such as the wave speed, is assumed to affect the apical and basal regions equally and not to affect other variables. If we were to alter the wave speed experimentally, perhaps by inhibiting the Ca^{2+} release channels, we might expect the profile of the oscillations at the two membranes to change. It is also likely that the frequency, amplitude and mean Ca^{2+} concentration would also be changed.

In Section 5 we consider the time-dependence of the Cl^{-} channel gating using the experimental data and model of Arreola et al. (1996). There are other time-dependent processes that have not been included in this analysis. As previously mentioned, further data is needed for the inclusion of time-dependent maxi-K channels. Membrane mechanics and fluid dynamics are also likely to add time-dependent effects to the model, but are not considered due to their complexity.

The overall aim of our research is to understand the regulation of saliva secretion across temporal and spatial scales from individual ion channels to whole gland secretion rates. To create a multiscale model of saliva secretion we must decide what detail to include and what to simplify. Given that Ca^{2+} waves are found experimentally, a spatial modelling approach might be taken using partial differential equations to solve for Ca^{2+}. However, unless we are particularly interested in how Ca^{2+} waves arise then this detailed spatial model will be numerically costly and produce large amounts of data which are not required. A conclusion from this analysis is that a detailed model of Ca^{2+} waves is unlikely to result in improved results relating to the rate of fluid secretion. By far the most important signalling mechanism is found to be the mean Ca^{2+} concentration. Therefore it is our opinion than a compartment model using ordinary differential equations with homogeneous Ca^{2+} oscillations is sufficient when considering secretion rate as the most important model variable. Going further, if mean secretion rate is the only model concern and extreme computational constraints existed, perhaps considering a whole-organ model, it would even be possible to ignore all oscillations completely and just consider Ca^{2+} as a constant function of agonist stimulation.

On the topic of signal transduction we might hypothesise that the process of salivation does not require the complex signal encoding that is seen in some other cell types. It seems unlikely that we must signal for an exact saliva secretion rate. If accuracy in the flow rate is not required then an increase in mean Ca^{2+} might be all that is required as a signalling mechanism. We might further hypothesise that the other experimentally observed wave properties, such as oscillation frequency and wave speed, might be tuned to values which offer the maximum efficiency in secretion for a given mean Ca^{2+} concentration.

Acknowledgments

This work was supported by National Institutes of Health Grant R01-DE19245.

References

Almassy J, Won J, Begenisich T, Yule D. Apical ca2+-activated potassium channels in mouse parotid acinar cells. The Journal of General Physiology. 2012; 139(2):121–133. [PubMed: 22291145]

Arreola J, Melvin J, Begenisich T. Activation of calcium-dependent chloride channels in rat parotid acinar cells. The Journal of General Physiology. 1996; 108(1):35–47. [PubMed: 8817383]

Ben-Aryeh H, Shalev A, Szargel R, Laor A, Laufer D, Gutman D. The salivary flow rate and composition of whole and parotid resting and stimulated saliva in young and old healthy subjects. Biochemical medicine and metabolic biology. 1986; 36(2):260–265. [PubMed: 2430601]

Berridge M. The AM and FM of calcium signalling. Nature. 1997; 386:759–760. [PubMed: 9126727]

Bruce JIE, Shuttleworth TJ, Giovannucci DR, Yule DI. Phosphorylation of inositol 1,4,5-trisphosphate receptors in parotid acinar cells. a mechanism for the synergistic effects of cAMP on Ca2+ signaling. J Biol Chem. 2002; 277(2):1340–1348. [PubMed: 11694504]

De Koninck P, Schulman H. Sensitivity of CaM kinase II to the frequency of Ca2+ oscillations. Science. 1998; 279(5348):227. [PubMed: 9422695]

Foskett J, Melvin J. Activation of salivary secretion: coupling of cell volume and [Ca2+]i in single cells. Science. 1989; 244(4912):1582–1585. [PubMed: 2500708]

Foskett JK. [Ca2+]i modulation of Cl- content controls cell volume in single salivary acinar cells during fluid secretion. AJP - Cell Physiology. 1990; 259(6):C998–1004.

Gin E, Crampin EJ, Brown DA, Shuttleworth TJ, Yule DI, Sneyd J. A mathematical model of fluid secretion from a parotid acinar cell. Journal of Theoretical Biology. 2007; 248(1):64–80. [PubMed: 17559884]

Goldbeter A, Dupont G, Berridge M. Minimal model for signal-induced Ca2+ oscillations and for their frequency encoding through protein phosphorylation. Proceedings of the National Academy of Sciences of the United States of America. 1990; 87(4):1461. [PubMed: 2304911]

Gray P. Oscillations of free cytosolic calcium evoked by cholinergic and catecholaminergic agonists in rat parotid acinar cells. The Journal of Physiology. 1988; 406(1):35. [PubMed: 3254416]

Heft M, Baum B. Basic biological sciences unstimulated and stimulated parotid salivary flow rate in individuals of different ages. Journal of dental research. 1984; 63(10):1182. [PubMed: 6592197]

Jaffe L. The path of calcium in cytosolic calcium oscillations - a unifying hypothesis. Proceedings of the National Academy of Sciences of the United States of America. Nov; 1991 88(21):9883–9887. [PubMed: 1946414]

Larsen A, Olsen L, Kummer U. On the encoding and decoding of calcium signals in hepatocytes. Biophysical chemistry. 2004; 107(1):83–99. [PubMed: 14871603]

Palk L, Sneyd J, Shuttleworth T, Yule D, Crampin E. A dynamic model of saliva secretion. Journal of Theoretical Biology. 2010

Sneyd J, Tsaneva-Atanasova K, Bruce JIE, Straub SV, Giovannucci DR, Yule DI. A model of calcium waves in pancreatic and parotid acinar cells. Biophysical Journal. 2003; 85(3):1392–1405. [PubMed: 12944257]

Takahata T, Hayashi M, Ishikawa T. SK4/IK1-like channels mediate TEA-insensitive, Ca2+-activated K+ currents in bovine parotid acinar cells. AJP - Cell Physiology. 2003; 284(1):C127–144. [PubMed: 12388063]

Tang Y, Othmer H. Frequency encoding in excitable systems with applications to calcium oscillations. Proceedings of the National Academy of Sciences. 1995; 92(17):7869.

Thompson J, Begenisich T. Membrane-delimited inhibition of maxi-K channel activity by the intermediate conductance Ca2+-activated K channel. J Gen Physiol. Feb; 2006 127(2):159–69. [PubMed: 16418402]

Won J, Cottrell W, Foster T, Yule D. Ca2+ release dynamics in parotid and pancreatic exocrine acinar cells evoked by spatially limited flash photolysis. American Journal of Physiology-Gastrointestinal and Liver Physiology. 2007; 293(6):G1166. [PubMed: 17901163]

Zimmermann B, Walz B. The mechanism mediating regenerative intercellular Ca2+ waves in the blowfly salivary gland. The EMBO journal. 1999; 18(12):3222–3231. [PubMed: 10369663]

Appendix A. Model equations

Appendix A.1. Fluid flow model

A summary of the main differential equations in the fluid flow model is included below. We use the following subscript notation with $[Cl]_i$, $[Cl]_l$ and $[Cl]_e$ denoting the Cl^- concentration in the cytosol, lumen and interstitium respectively. For full details and

parameter values see Palk et al. (2010), we choose to not include apical K^+ channels in this analysis and therefore set $\alpha_K = 1$. Differential equations for the cytosolic concentrations are as follows,

$$\frac{d([\mathrm{Cl}]_i w)}{dt} = -\frac{I_{\mathrm{Cl}}}{z_{\mathrm{Cl}} F} + 2J_{\mathrm{NKCC}}, \tag{A.1}$$

$$\frac{d([\mathrm{Na}]_i w)}{dt} = -3J_{\mathrm{Nak}} + J_{\mathrm{NKCC}}, \tag{A.2}$$

$$\frac{d([\mathrm{K}]_i w)}{dt} = 2J_{\mathrm{NaK}} + J_{\mathrm{NKCC}} - \frac{I_{\mathrm{K}}}{z_{\mathrm{K}} F}, \tag{A.3}$$

where

$$I_{\mathrm{tight}} = \frac{V_a - V_b}{R_{\mathrm{tight}}},$$

is the current through the tight junction.

Lumenal ionic concentrations are given by the following differential equations,

$$w_L \frac{d([\mathrm{Na}]_l)}{dt} = \frac{g_{\mathrm{t,Na}} I_{\mathrm{tight}}}{z_{\mathrm{Na}} F} - q_{\mathrm{tot}} [\mathrm{Na}]_l, \tag{A.4}$$

$$w_L \frac{d([\mathrm{K}]_l)}{dt} = \frac{(1 - g_{\mathrm{t,Na}}) I_{\mathrm{tight}}}{z_{\mathrm{K}} F} - q_{\mathrm{tot}} [\mathrm{K}]_l, \tag{A.5}$$

$$w_L \frac{d([\mathrm{Cl}]_l)}{dt} = \frac{I_{\mathrm{Cl}}}{z_{\mathrm{Cl}} F} - q_{\mathrm{tot}} [\mathrm{Cl}]_l. \tag{A.6}$$

Equations for the basal and apical membrane potentials are,

$$C_m \frac{dV_b}{dt} = -I_{\mathrm{K}} - F J_{\mathrm{NaK}} + I_{\mathrm{tight}}, \tag{A.7}$$

$$C_m \frac{dV_a}{dt} = -I_{\mathrm{Cl}} - I_{\mathrm{tight}}. \tag{A.8}$$

The fluid flow across the apical membrane is

$$q_a = RTL_{\mathrm{Pa}} \left([\mathrm{Cl}]_l + [\mathrm{Na}]_l + [\mathrm{K}]_l - \left([\mathrm{Cl}]_i + [\mathrm{Na}]_i + [\mathrm{K}]_i + [\mathrm{Ca}]_i + \frac{x}{w} \right) \right),$$

were $[Ca]_i$ is the mean Ca^{2+} concentration throughout the cytosol given by

$$[\mathrm{Ca}]_i=\frac{C_a+C_b}{2},$$

where C_a and C_b are the apical and basal Ca^{2+} concentrations respectively.

The basal fluid flow q_b and paracellular fluid flow q_{tight} are given respectively,

$$q_a=RTL_{\mathrm{Pb}}\left([\mathrm{Cl}]_i+[\mathrm{Na}]_i+[\mathrm{K}]_i+[\mathrm{Ca}]_i+\frac{x}{w}-([\mathrm{Cl}]_e+[\mathrm{Na}]_e+[\mathrm{K}]_e)\right),$$

$$q_{\mathrm{tight}}=RTL_{\mathrm{Pt}}([\mathrm{Cl}]_l+[\mathrm{Na}]_l+[\mathrm{K}]_l-([\mathrm{Cl}]_e+[\mathrm{Na}]_e+[\mathrm{K}]_e)).$$

The total secretion is then given by the sum of the paracellular and transcellular components,

$$q_{\mathrm{tot}}=q_a+q_{\mathrm{tight}}.$$

The cell volume is governed by the balance of incoming and outgoing fluid flow,

$$\frac{dw}{dt}=qb-qa. \tag{A.9}$$

Full details of the fluxes and parameters used can be seen in Palk et al. (2010).

Appendix A.2. Cl^- channels

For the analysis in Section 4 a steady-state model of Cl^- channel gating from Arreola et al. (1996) is used (for details of the non steady-state model see Section 5). Here the Cl^- channel steady-state open probability is given as

$$P_{\mathrm{Cl}}=\frac{1}{1+K_2(K_1^2/C_a^2+K_1/C_a+1)}.$$

Where C_a is the Ca^{2+} concentration at the apical membrane and

$$K_1=214\exp\left(\frac{-0.13FV_a}{RT}\right)nM,$$

$$K_2=0.58\exp\left(\frac{-0.24FV_a}{RT}\right).$$

Here V_a is the membrane potential of the apical membrane. Total current through the Cl^- channels is then given by,

$$I_{\mathrm{Cl}} = g_{\mathrm{cl}} P_{\mathrm{Cl}} (V_a - V_{\mathrm{Cl}})$$

g_{Cl} is the maximum whole cell conductance, 31.4 nS found by Arreola et al. (1996). V_{Cl} is the Nernst potential given by,

$$V_{\mathrm{Cl}} = \frac{RT}{z_{\mathrm{Cl}} F} \log\left(\frac{[\mathrm{Cl}]_l}{[\mathrm{Cl}]_i}\right)$$

$z_{\mathrm{Cl}} = -1$ is the valence of Cl^-, $R = 8.315$ J mol^{-1} K^{-1}, $T = 310$ K and $F = 96490$ C mol^{-1}.

Appendix A.3. K^+ channels

We use the model of Takahata et al. (2003). The steady-state open probability of the K^+ channel at the basal membrane is given as,

$$P_K = \frac{1}{1 + (K_d / C_b)^{nH}}$$

where C_b is the Ca^{2+} concentration at the basal membrane and $nH = 2.54$ and $K_d = 0.182$ μM. K_d is modified from the value found by Takahata et al. (2003) of $K_d = 0.43$ μM to give a small open probability at steady state Ca^{2+} concentrations.

The current through the K^+ channel at the basolateral membrane, I_K, is given by

$$I_{\mathrm{K}} = g_K P_K (V_b - V_{\mathrm{K}})$$

where g_K is the maximum whole cell conductance of 14 nS, the value found by Thompson and Begenisich (2006). V_K is the nernst potentials of the basololatoral membrane given by,

$$V_{\mathrm{K}} = \frac{RT}{z_K F} \log\left(\frac{[\mathrm{K}]_e}{[\mathrm{K}]_i}\right)$$

here $z_K = +1$ is the valence of K^+.

Appendix A.4. Na^+ - K^+ - ATPase simplification

As in Palk et al. (2010) a simplified model of the Na^+ - K^+ - ATPase is used with the steady-state flux as follows.

$$\nu_{\mathrm{NaK}} = r\frac{[K]_e^2[\mathrm{Na}]_i^3}{[K]_e^2+\alpha[\mathrm{Na}]_i^3} \tag{A.10}$$

With $r = 1.305 \times 10^6\ \mathrm{s}^{-1}\ \mathrm{mM}^{-3}$ and $\alpha = 0.647\ \mathrm{mM}^{-1}$. $J_{\mathrm{NaK}} = a_{\mathrm{NaK}}\nu_{\mathrm{NaK}}$, where $a_{\mathrm{NaK}} = 2.236 \times 10^{-17}$ mol is the density of the Na^+ - K^+ - ATPase exchanger.

Appendix A.5. Na^+ - K^+ - $2Cl^-$ cotransporter simplification

As in Palk et al. (2010) a simplified model of the Na^+ - K^+ - $2Cl^-$ cotransporter is used with the steady-state flux as follows.

$$\nu_{\mathrm{NKCC}} = r_{\mathrm{NKCC}}\frac{1-\alpha_1[\mathrm{Na}]_i[K]_i[\mathrm{Cl}]_i^2}{K_{\mathrm{NKCC}}+\alpha_2[\mathrm{Na}]_i[K]_i[\mathrm{Cl}]_i^2} \tag{A.11}$$

Where $r_{\mathrm{NKCC}} = 4.31\ \mathrm{s}^{-1}$, $\alpha_1 = 1.2755 \times 10^5$, $\alpha_2 = 3.7894 \times 10^4$ and $K_{\mathrm{NKCC}} = 0.0282\ \mathrm{mM}^4$. $J_{\mathrm{NKCC}} = \nu_{\mathrm{NKCC}}a_{\mathrm{NKCC}}$ where $a_{\mathrm{NKCC}} = 3.2 \times 10^{-17}$ mol is the membrane density of the cotransporter.

Appendix B. Approximate analysis of model equations: synchronous Ca2+ waves produce a local maximum for fluid secretion

Here we seek to show that the fluid secretion model with steady-state ion channels seen in Section 2 has a maximum secretion rate when Ca^{2+} oscillations are synchronous at apical and basal membranes. In order to do this we must make some assumptions. First we make the assumption that the membrane potentials are at quasi-steady-state, which we can justify given the very small membrane capacitance C_m. This gives,

$$C_m\frac{dV_a}{dt} = -I_{\mathrm{Cl}} - I_{\mathrm{tight}} = 0 \tag{B.1}$$

and

$$C_m\frac{dV_b}{dt} = -I_K - FJ_{\mathrm{Nak}} + I_{\mathrm{tight}} = 0. \tag{B.2}$$

Now we substitute the definitions for the currents, I_K, I_{Cl} and I_{tight} into equations B.1 and B. 2, giving,

$$-g_{\mathrm{cl}}P_{\mathrm{cl}}(V_a - V_{\mathrm{Cl}}) = (V_a - V_b)/R_{\mathrm{tight}}$$

and

$$g_kP_k(V_b - V_k) + FJ_{\mathrm{Nak}} = (V_a - V_b)/R_{\mathrm{tight}}.$$

If we solve both these equations simultaneously we can get expressions for the membrane potentials V_a and V_b. During simulations it is found that, for near isosmotic fluid secretion,

fluid flow is proportional to the current through the tight junction, see Maclaren et al., 2011 (in submission). The tight junctional current is given by $(V_a - V_b)/R_{tight}$, we use this as follows.

$$flow \propto \frac{V_a - V_b}{R_{\text{tight}}} = \frac{P_{\text{CL}} P_K (V_{\text{Cl}} - V_k) + P_{\text{CL}} F J_{\text{Nak}}}{P_K + P_K R_{\text{tight}} P_{\text{CL}} + P_{\text{CL}}}$$

Here we have used the notations $P_{\text{CL}} = P_{\text{cl}} g_{\text{Cl}}$ and $P_K = P_k g_k$.

Appendix B.1. Periodic functions

We will make the assumption that during the course of one Ca^{2+} wave both P_{CL} and P_K are periodic functions. We take this assumption further to make these both the same periodic function with a phase difference δ. We also assume V_{Cl} and V_k stay approximately constant, a valid assumption if changes in ionic concentrations are small. We then denote, $f(t) = \frac{1}{P_K (V_{\text{Cl}} - V_k)}$, $f(t+\delta) = \frac{1}{P_{\text{CL}} (V_{\text{Cl}} - V_k)}$, $\gamma = F J_{\text{Nak}}$ and $A = \frac{R_{\text{tight}}}{(V_{\text{Cl}} - V_k)}$. The expression for fluid flow then becomes,

$$flow \propto \frac{1 + \gamma f(t)}{f(t) + f(t+\delta) + A},$$

where A and γ are positive constants and $f(t)$ is any periodic function, period T. Now we would like to see how the average flow over the course of one period, T, depends on the phase difference δ.

We define I to be the total flow over a period, T,

$$I = \int_0^T \frac{1 + \gamma f(t)}{A + f(t) + f(t+\delta)} dt.$$

We would like to find when this expression has a maximum and minimum. Taking the derivative with respect to δ,

$$\frac{\partial I}{\partial \delta} = -\int_0^T \frac{(1 + \gamma f(t)) f'(t+\delta)}{(A + f(t) + f(t+\delta))^2} dt.$$

We predict a maximum at $\delta = 0$, so looking at the partial derivate here,

$$\frac{\partial I}{\partial \delta}\Big|_{\delta=0} = -\int_0^T \frac{(1 + \gamma f(t)) f'(t)}{(A + 2f(t))^2} dt = \frac{1}{2(A + 2f(t))} - \frac{\gamma}{4} \ln(2f(t) + A) - \frac{\gamma A}{4(2f(t) + A)}\Big|_0^T.$$

As, $2f(0) = 2f(T)$, being a periodic function, this gives,

$$\frac{\partial I}{\partial \delta}\Big|_{\delta=0}=0$$

and therefore a maximum or minimum occurs when there is no phase difference. To determine whether this is a maximum or minimum we look at the second derivative.

$$\frac{\partial^2 I}{\partial \delta^2}\Big|_{\delta=0}=-\int_0^T \frac{(1+\gamma f(t))f''(t)}{(A+2f(t))^2}dt+2\int_0^T \frac{(1+\gamma f(t)))(f'(t))^2}{(A+f(t))^3}dt \equiv I_1+I_2+I_3+I_4$$

where,

$$I_1=\int_0^T \frac{-f''(t)}{(A+2f(t))^2}dt$$
$$I_2=2\int_0^T \frac{(f'(t))^2}{(A+f(t))^3}dt.$$
$$I_3=\int_0^T -\frac{\gamma f(t)f''(t)}{(A+2f(t))^2}$$

and

$$I_4=\int_0^T \frac{2\gamma f(t)(f'(t))^2}{(A+2f(t))^3}$$

Evaluating the first integral, I_1 using integration by parts,

$$I_1=-\frac{f'(t)}{(A+2f(t))^2}\Big|_0^T-\int_0^T \frac{4(f'(t))^2}{(A+2f(t))^3}dt=0-4\int_0^T \frac{(f'(t))^2}{(A+2f(t))^3}dt.$$

Evaluating the integral I_3 using integration by parts,

$$I_3=\int_0^T -\frac{\gamma f(t)f''(t)}{(A+2f(t))^2}=-\frac{\gamma f(t)f'(t)}{(A+2f(t))^2}\Big|_0^T+\int_0^T \frac{\gamma(f'(t))^2}{(A+2f(t))^2}dt-\int_0^T \frac{4\gamma f(t)(f'(t))^2}{(A+2f(t))^3}dt$$
$$=0+\int_0^T \frac{\gamma(f'(t))^2}{(A+2f(t))^2}dt-\int_0^T \frac{4\gamma f(t)(f'(t))^2}{(A+2f(t))^3}dt$$

Now

$$\frac{\partial^2 I}{\partial \delta^2}\Big|_{\partial=0}=-\int_0^T \frac{2(f'(t))^2}{(A+2f(t))^3}dt-\int_0^T \frac{2\gamma f(t)(f'(t))^2}{(A+2f(t))^3}dt+\int_0^T \frac{\gamma(f'(t))^2}{(A+2f(t))^2}dt$$
$$=-(2-\gamma A)\int_0^T \frac{(f'(t))^2}{(A+2f(t))^3}dt$$

If we assume A is a positive constant and that $f(t)$ is a positive function, both valid assumptions, then here we are taking the integral of an expression that is strictly positive. The sign of the second derivative is therefore determined by the expression $(2 - \gamma A)$.

Looking back to the original notation, $\gamma A = F J_{\text{Nak}} \frac{R_{\text{tight}}}{(V_{\text{Cl}} - V_k)}$. Under physiological condition the various terms are of the following magnitude,

$$(V_{\text{Cl}} - V_{\text{K}}) \sim O(10^{-2}),$$
$$R_{\text{tight}} \sim O(10^{8}),$$
$$F J_{\text{Nak}} \sim O(10^{-12}).$$

Therefore $\gamma A \sim O(10^{-2})$ and,

$$\frac{\partial^2 I}{\partial \delta^2}\Big|_{\delta=0} = -(2-\gamma A)\int_0^T \frac{(f'(t))^2}{(A+2f(t))^3} dt < 0.$$

By proving the second derivative is negative we have shown that $\delta = 0$ is a local maximum and thus there is a local maximum in secretion when Ca^{2+} waves are synchronous at the apical and basal membranes.

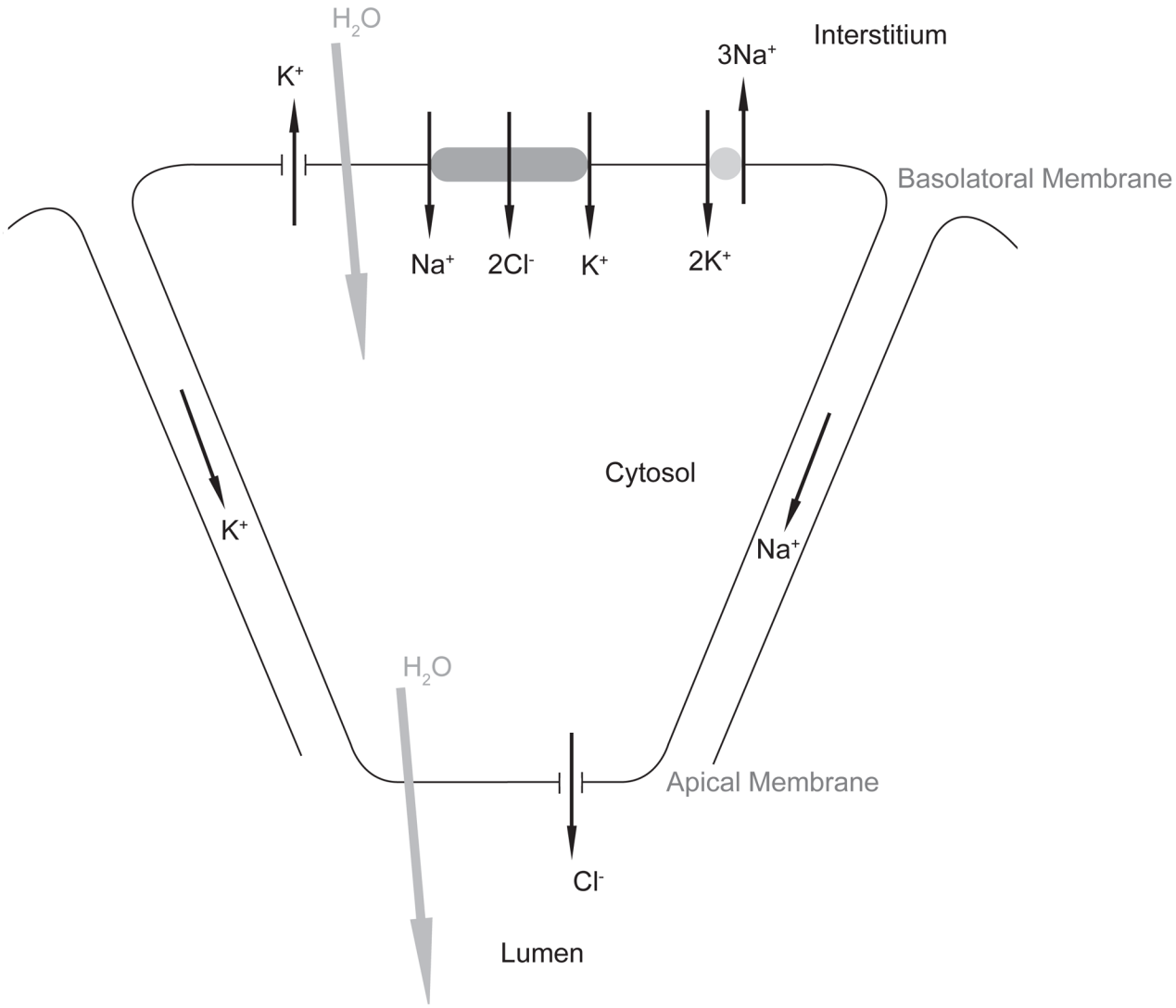

Figure 1.
A schematic of the movement of ions responsible for saliva secretion

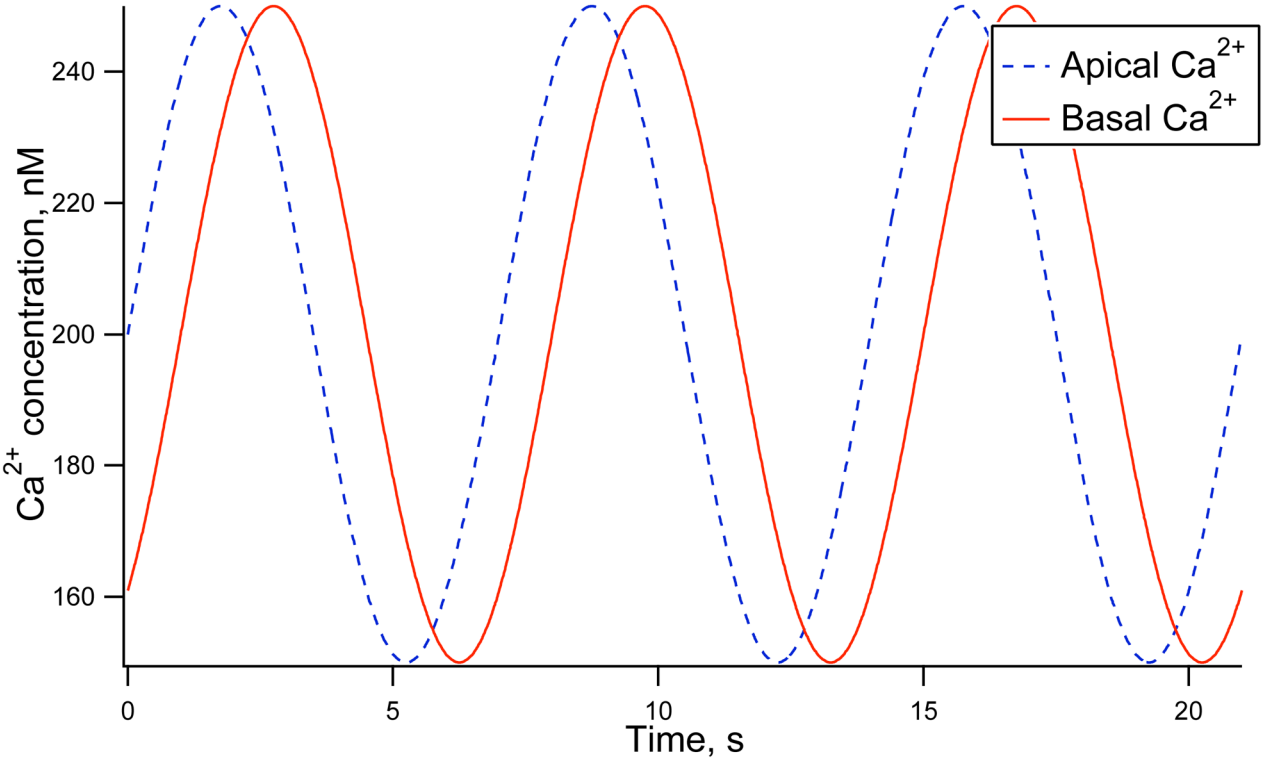

Figure 2.
Ca^{2+} concentrations at the apical and basal membrane numerically simulated with sine waves, period 7 s, with mean 200 nM and 50 nM amplitude. There is a 1 s time difference between the apical and basal Ca^{2+} peak which is equivalent to a 25 μm/s wave speed.

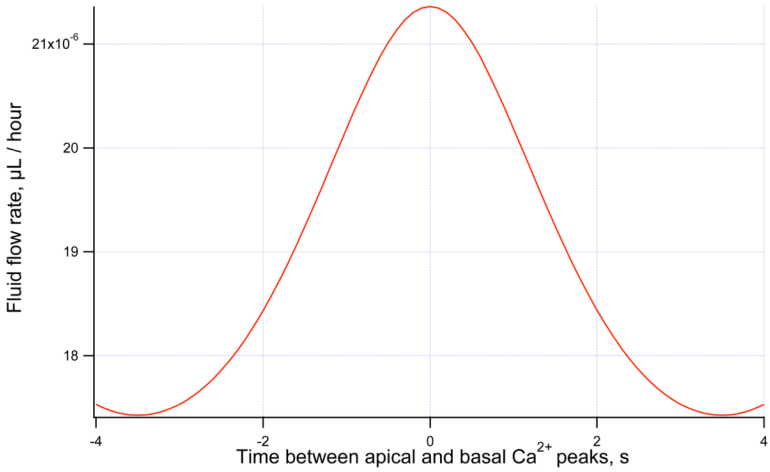

Figure 3.

Fluid flow rate against time difference between apical and basal Ca^{2+} peak. Maximum secretion occurs when the apical and basal oscillations are synchronous. Ca^{2+} waves are approximated using a sine function with 150 nM mean, 100 nM amplitude and 7 s period.

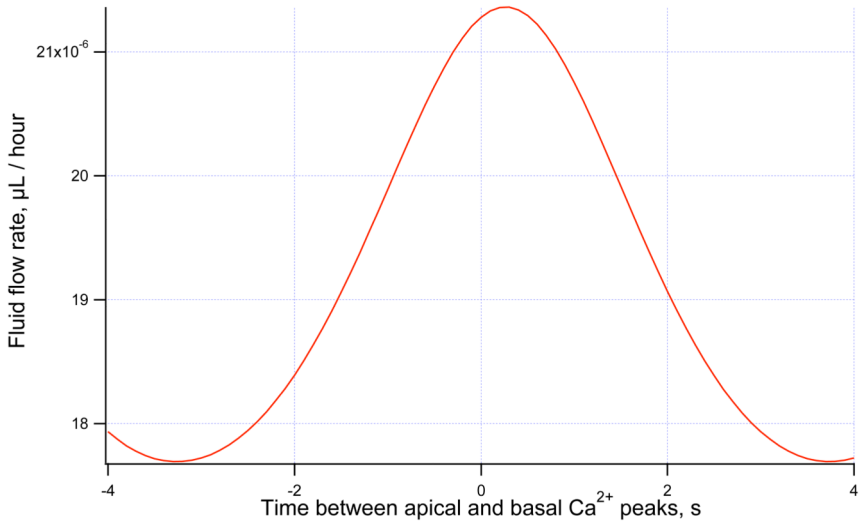

Figure 4.

Fluid flow rate against time difference between apical and basal Ca^{2+} peak in a model with time-dependent Cl^- channels. Maximum fluid flow occurs when Ca^{2+} peaks at the apical membrane 0.2 s before the basal membrane.

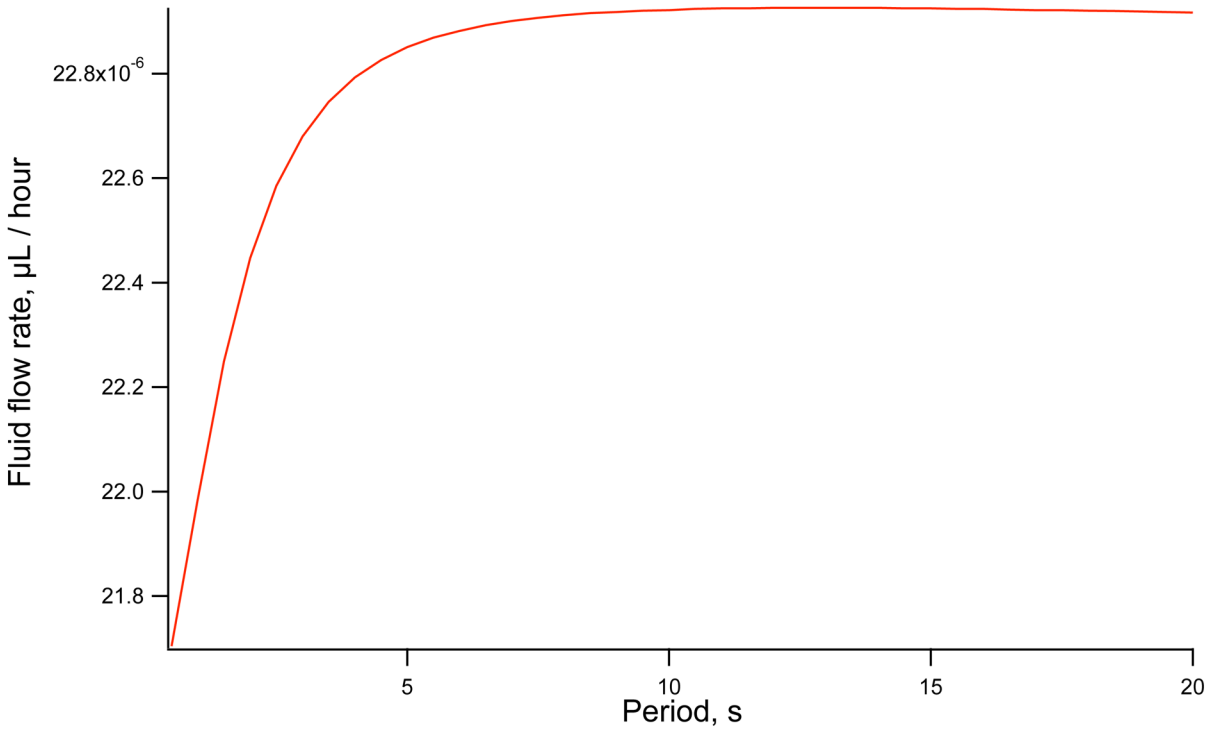

Figure 5.
Fluid flow rate against period of Ca^{2+} oscillations. The maximum fluid flow rate occurs with long period oscillations.

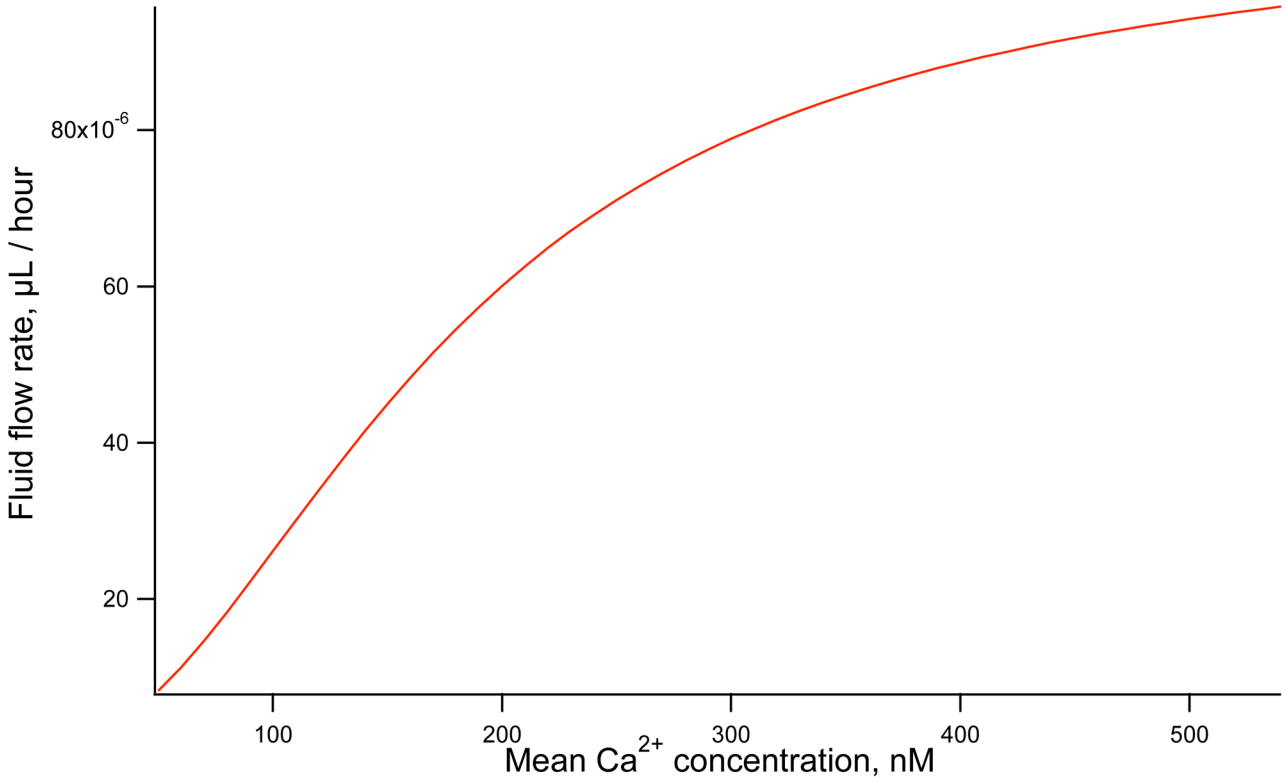

Figure 6.
Fluid flow rate against mean Ca^{2+} concentration. Larger mean Ca^{2+} concentrations increase secretion rate. Simulations are completed using a sine function with 20 nM amplitude and 7 s period.

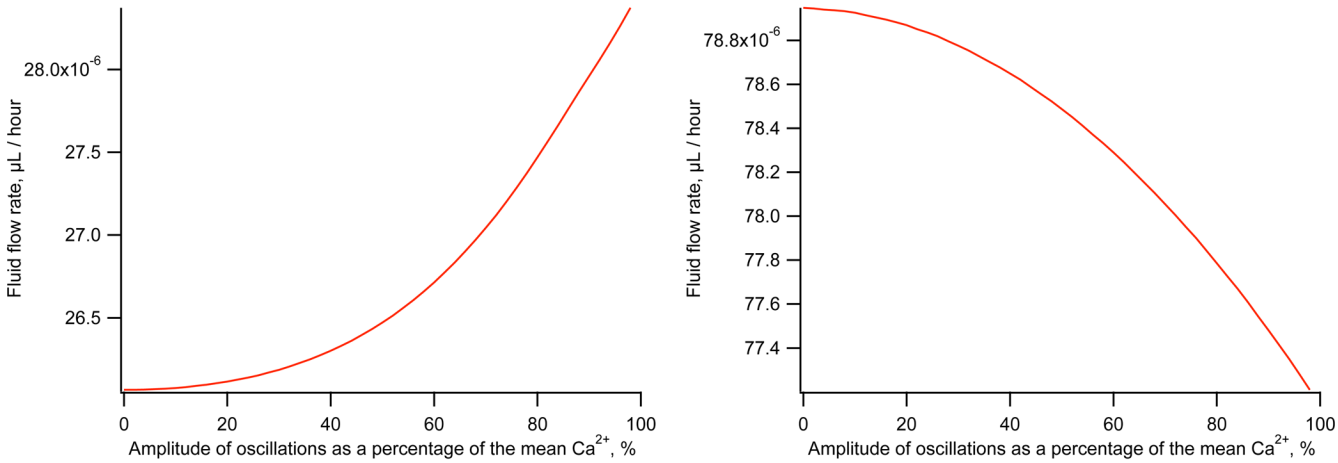

(a) 100 nM mean Ca^{2+} (b) 300 nM mean Ca^{2+}

Figure 7.

Fluid flow rate against amplitude of periodic Ca^{2+} oscillations for two different mean Ca^{2+} concentrations. The maximum fluid flow rate occurs with large amplitude oscillations for a 100 nM mean Ca^{2+}. With a larger 300 nM mean Ca^{2+} the maximum secretion occurs with low amplitude oscillations. Both simulations are completed with a 7 s period sine function.

J Theor Biol. Author manuscript; available in PMC 2013 July 21.

Table A.1

Model parameter values

Physical constants					
R	8.315 J mol^{-1} K^{-1}	T	310 K	F	96490 C mol^{-1}
Whole cell conductance's					
g_{Cl}	31.4 nS *	g_K	14 nS **		
Pump Densities					
α_{NaK}	2.236×10^{-17} mol	α_{NKCC}	3.2×10^{-17} mol		
Volumes					
w_0	10^{-12} L	w_L/w_0	0.02		
Water permeabilities					
L_{Pa}	1.68×10^{-15} L^2 J^{-1} s^{-1}	L_{Pb}	2.07×10^{-14} L^2 J^{-1} s^{-1}		
L_{Pt}	8.4×10^{-17} L^2 J^{-1} s^{-1}				
Cell properties					
C_m	$10^{-11}F$	x/w_0	30.7 mM		
Electrical parameters					
R_t	6.8×10^8 ohms	$g_{t,Na}$	0.955		
Ionic valence					
z_{Cl}	−1	z_K	+1	z_{Na}	+1
Interstitial concentrations					
$[Cl]_e$	102.6 mM	$[Na]_e$	140.2 mM	$[K]_e$	5.3 mM

* from Arreola et al. (1996),

** from Thompson and Begenisich (2006), other parameters are physical constants or model fits chosen to give the correct steady state concentrations and membrane potentials.